Indonesian Journal of Maritime Technology (ISMATECH)
Vol. 2, Issue 2, December 2024
eISSN: 3025-518X
DOI: https://doi.org/10.35718/ismatech.v2i2.1228

CFD-Preliminary Design and Stability Analysis of a High-Speed Firefighting Boat for Remote Island Waterways

Moh.Winki Wirawan[1], Achdri Fauzi Nugraha Oloan[1*], Albert Gabriel Surbakti[1], Joan Rike Batosai[2]

[1]Department of Ship Manufacturing Engineering, Politeknik Negeri Banyuwangi, Kabat, Banyuwangi, 68461, Indonesia
[2]Department of Naval Architecture, Institut Teknologi Sepuluh Nopember, Surabaya, 60111 Indonesia

KEYWORDS
Firefighting Vessel
Ship Resistance
CFD Simulation
Stability Analysis

ABSTRACT – The Seribu Islands, administered by the DKI Jakarta Provincial Government, cover an area of 4,745.62 km², with 8.76 km² of land spread across two sub-districts and six major islands: Kelapa, Harapan, Panggang, Tidung, Pari, and Untung Jawa. While these islands are popular tourist destinations with adequate transport facilities, the remote, water-surrounded nature of the area poses challenges for emergency response, particularly firefighting. To address this, the authors designed a firefighting vessel optimized for quick deployment and effective fire suppression. The design process focused on determining optimal dimensions and minimizing hydrodynamic resistance through hull variation using effect of length on resistance method, followed by exponential regression. The vessel's main dimensions are LOA 16.5 m, LPP 15.588 m, beam 4.9 m, depth 2.5 m, draft 0.9 m, and a top speed of 36 knots. Four hull configurations with varying chine type and angles (0°, 10°, and 17°) were simulated in Numeca Fine Marine (CFD) and Maxsurf. The third hull variation achieved the lowest resistance, with a resistance value of 67.12 kN. Equipped with a pump capacity of 474 m³/h and a spray range of 25 m, the vessel provides effective firefighting capabilities. Stability analysis, including fire monitor placement variations, indicates the optimal trim and stability with a Max GZ angle of 50° and a roll period of 3.14 seconds. This design demonstrates a feasible solution for firefighting within the Seribu Islands' unique aquatic environment.

*Corresponding Author | Achdri Fauzi Nugraha Oloan | ✉ achdri@poliwangi.ac.id

INTRODUCTION

The Seribu Islands are a distinctive archipelago within the Jakarta region, known for their popularity as a coastal retreat and recreational destination as shown in Figure 1 [1]. With tourism on the rise, the islands attract thousands of visitors who rely heavily on boat transport to explore the area [2]. This high volume of maritime traffic, however, brings heightened risks, particularly concerning onboard fire hazards [3]. The reliance on waterborne travel creates a unique challenge for emergency response, as effective firefighting requires specialized equipment and vessels capable of quick deployment across open waters. Currently, response resources are predominantly based onshore, leading to delayed assistance in critical situations where immediate action is necessary.

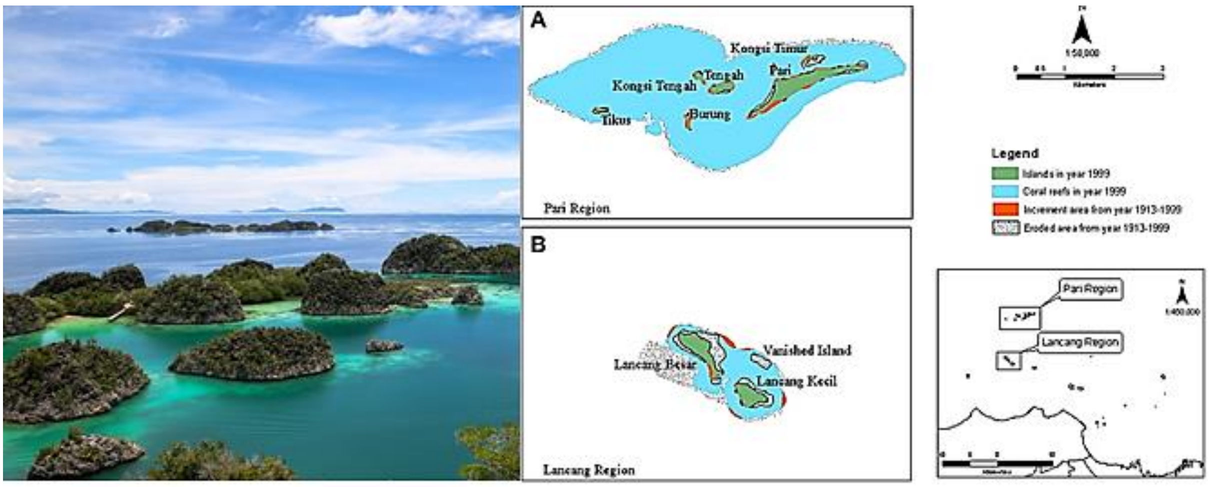

Figure 1. Typical Mapping of Seribu Island, Jakarta, Indonesia [1].

Previous research has explored various aspects of firefighting vessel design and safety measures in island and marine environments, focusing on vessel stability, hydrodynamic resistance, and emergency response efficiency [4]. However, existing designs have not fully addressed the unique requirements of high-speed firefighting vessels with optimized hulls suited to the Seribu Islands' geographical and environmental context [5]. Recent advancements in computational fluid dynamics (CFD) have facilitated more precise analyses of hydrodynamic resistance and stability, particularly for high-speed vessels equipped with specialized firefighting equipment [6]. This study differentiates itself by employing CFD simulations and Maxsurf software to develop and test multiple hull configurations, aiming to identify an optimal design with minimal resistance, enhanced stability, and robust firefighting capabilities [7], [8].

The primary objective of this research is to design a high-speed firefighting vessel for the Seribu Islands, addressing the need for effective firefighting response and enhanced tourist safety. The study's findings are expected to contribute valuable insights into emergency vessel design, offering practical applications for tourist regions facing similar logistical and safety challenges.

METHOD

The research methodology for this study, which focuses on designing a specialized fireboat for emergency accessibility within the waters of the Seribu Islands, encompasses a structured approach to data acquisition, modeling, analysis, and validation, ultimately aimed at achieving a functional and effective fire response vessel. Initially, the research object, defined as the fireboat capable of rapid deployment and response within the archipelagic region, requires primary data collection, specifically regarding the design concept and crucial specifications [9]. The data collection phase, which establishes the foundational design elements, involves a systematic acquisition of essential data, including core design concepts that form the basis for the fireboat's layout and structural efficiency during firefighting operations. This involves the creation of preliminary sketches, detailed technical drawings, and explicit design statements to convey the functionality and purpose of each design aspect [10].

In the design stage, a comprehensive three-part approach was adopted, encompassing the construction of a lines plan, the general arrangement, and the propulsion system selection, as well as the development of a 3D model. The lines plan, representing the vessel's hull projection, was developed to provide clarity on the hull's contours and structural design. Concurrently, the general arrangement was configured to capture essential layout perspectives from the vessel's side, top, and front, offering a multidimensional view crucial for further stability analysis and operational planning [11], [12]. Propulsion system selection was carefully considered to identify an optimal engine and propulsion type, ensuring the vessel's operational efficiency and performance within coastal and nearshore environments. A 3D model was then constructed to visually demonstrate the conceptual design, offering an integrated and realistic depiction of the vessel's anticipated physical form and layout.

With the initial design parameters established, the study transitioned into the treatment phase, where the research object (the fireboat hull and associated stability mechanisms) was tested across multiple variations to assess stability and resistance. Total ship resistance is defined as the counteracting force that a vessel faces when moving, generated by the frictional interaction between the hull and the surrounding water. Key contributors to ship resistance include viscous resistance, which is notably influenced by the fluid's viscosity [13]-[15]. Viscous resistance itself comprises two main components: frictional resistance and form resistance, the latter resulting from the ship's hull shape. Ship model test trials require the use of specialized experimental facilities known as "towing tanks." In these trials, a three-dimensional scaled model of the ship is created using a geometric similarity scale, denoted as λ, to replicate the ship's shape for resistance analysis. This model is then towed through calm water in the tank to determine resistance values. In this setup, the total resistance R_T of the model is separated into frictional resistance and residual resistance, following the principles established by Froude in 1872 [16]. The total resistance, is represented in Equation 1 as follows:

$$R_T = C_T \times 0.5 \times \rho \times v_s{}^2 \times S \tag{1}$$

where CT is the total coefficient of resistance, ρ is sea water density, vs is the ship's service speed, and S is wetted surface area.

Specific variables were isolated for controlled testing, wherein the hull form and primary dimensions were maintained as fixed variables, ensuring consistency and relevance across each analysis. The independent variable in this stage, the placement of the fire monitor nozzle, was modified through multiple configurations to evaluate its effect on the fireboat's stability under simulated firefighting scenarios [17], [18]. This configuration testing allowed the study to capture varying stability responses as influenced by nozzle placement, offering data on ideal configurations for enhanced operational safety and efficiency.

The hull and vessel structure data input and modeling were conducted using Maxsurf Enterprise software, applying the ship resistance calculation theory commonly used in the shipbuilding industry, specifically the Holtrop method [16], following a detailed procedure that began with surface creation through the "Add Surface" feature, allowing for the foundational structural representation within the software environment. Following this, surfaces were duplicated to achieve the desired hull shape, with each surface aligned and merged using the bound edge command. This initial modeling was crucial to establishing a realistic simulation of the vessel's body. The shape of the hull was further refined by adjusting control points across the surface model, allowing for precision in forming the desired contours, curves, and structural lines that define the fireboat's hull.

To analyze the hull's performance in terms of resistance, the study used Maxsurf's capabilities not only to model the hull but also to simulate and capture relevant performance metrics, particularly the resistance or drag exerted on the hull. This resistance analysis provided a foundational metric for validating the design's efficiency, with the resistance values subsequently cross-validated against Computational Fluid Dynamics (CFD) software simulations, offering a robust comparison and validation point to ensure accuracy and reliability of the Maxsurf-based findings. To verify the precision of our CFD simulation, we conducted a convergence assessment by tracking the reduction in residuals as shown in Figure 2. A substantial and consistent decrease in residuals with increasing iterations generally indicates that the solution is approaching convergence, following principles established by Froude [6].

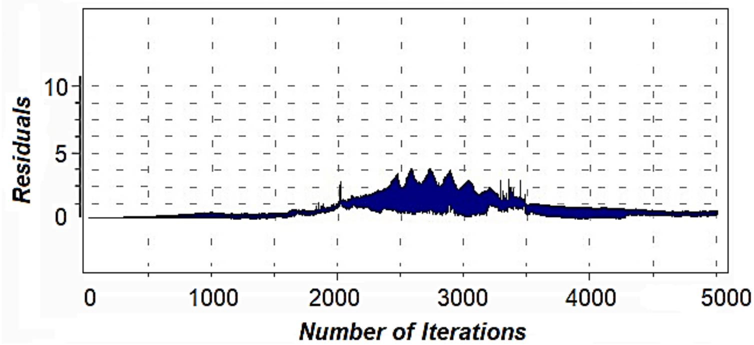

Figure 2. The Convergence Residuals Observed in our CFD Model.

Additionally, stability was analyzed through simulations assessing variations in righting arm (GZ) values and roll period across different placements of the fire monitor nozzle on the vessel, in accordance with International Maritime Organization (IMO) standards [19], see Figure 3 and Equation 2. This stage of the methodology provided essential data regarding the vessel's stability across operational scenarios, with each placement tested and evaluated to derive the most stable configuration that still meets firefighting functional requirements. This stability analysis, which assessed the response of the fireboat's stability mechanisms to nozzle configurations, offers insight into the vessel's suitability and reliability under the dynamic conditions likely to be encountered during emergency firefighting tasks in the Seribu Islands area.

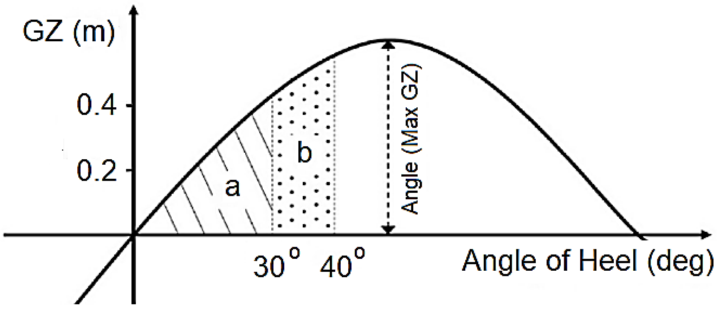

Figure 3. GZ Curve [19].

Key parameters related to the GZ curve include GZ30°, which indicates the righting arm at a 30° heel, and angle max GZ, the angle where the righting arm reaches its maximum. Figure 3, presents three areas beneath the GZ curve: Area 30° represents the area "a" from 0 to 30 degrees; Area 30, 40 deg, area "b" from 30 to 40 degrees (or the flooding angle, whichever is smaller); and Area 40°, which combines areas "a" and "b" from 0 to 40 degrees (or the flooding angle, if smaller). These areas are critical for evaluating the vessel's stability under various conditions, including the influence of wind and wave action. The heeling angle (angle passenger) caused by passenger crowding on one side must not exceed 10 degrees and can be calculated using Equation 2. This study applied the Korean Government's regulations for calculating the heeling angle [20]. The method employs a simplified empirical formula, allowing for straightforward results based solely on the ship's basic dimensions.

$$M_P = \frac{0.214\ kNm^2 \sum\left(\frac{7}{m^2} - \frac{n}{q}\right) n \times b}{100} \tag{2}$$

where M_P is the heeling moment caused by passengers (kNm), n is the number of passengers at each seating location, a is the floor area at each seating location (m²), and b is the average lateral movement distance of passengers in accessible areas (m).

The application of Equation 2 is employed to establish the stability criteria in accordance with the guidelines outlined in the IMO A.749 Code on Intact Stability, which provides a comprehensive framework for assessing the stability performance of vessels under various operational conditions and ensures compliance with international maritime safety standards.

In concluding the methodology, the study synthesized the findings from the design and simulation phases to present recommendations on optimal nozzle placement, along with design insights that enhance the fireboat's accessibility and response capabilities. By emphasizing responsive configuration and stability under load, this research aims to contribute to the literature on remote island firefighting solutions, particularly for challenging island geographies where terrestrial firefighting resources are often inadequate. As such, the fireboat design proposed through this study is intended as a reference for future applications in remote or hard-to-reach locations, enabling swift and effective responses to emergencies in coastal or island communities.

CFD Simulation

Based on the Navier–Stokes equations, the ISIS flow solver (NUMECA FINE Marine) numerically determines flow properties such as pressure, velocity, and density [21]. When considering incompressible flow, these equations, combined with the time continuity equation, can be expressed as follows:

$$\frac{\partial u_i}{\partial xi} = 0 \tag{3}$$

$$\frac{\partial u_i}{\partial t} + \frac{\partial\left(u_i u_j + u_i^{"} u_j^{"}\right)}{\partial x_i} = R_i - \frac{1}{\rho} \times \frac{\partial p}{\partial x_i} + \frac{\partial}{\partial x_j}\left(v\left(\frac{\partial u_i}{\partial x_j} + \frac{\partial u_j}{\partial x_i}\right)\right) \tag{4}$$

$$\mathrm{v} = \frac{\mu}{\rho} \tag{5}$$

where u_i is components of the time-averaged velocity along cartesian axes, x_i is cartesian coordinates, t is time, R_i is volume force, p is time-averaged pressure, ν is kinematic viscosity, μ is dynamic viscosity, and ρ is density.

By solving the mass conservation equation along with Newton's second law, also known as the momentum conservation equation, we can obtain the velocity and pressure fields.

For the mass conservation:

$$\frac{d}{dt}\iiint_D \rho dv = 0 \tag{6}$$

where D is the fluid domain, dv is an arbitrary control of volume.

For the momentum conservation:

$$\frac{d}{dt}\iiint_D \rho\vec{U} dv = \iiint_D \rho\overrightarrow{f_v} dv + \iint_D \vec{T} dS \tag{7}$$

where $\overrightarrow{f_v}$ is volume force (normally gravity force), S is the strain rate, and $\vec{T}$ is a constraint, i.e., $\vec{T} = \sigma \times \vec{n}$, where σ is the constraint tensor and $\vec{n}$ is the unit normal vector

Designed specifically for naval architecture, NUMECA's FINE Marine software includes three core modules that support comprehensive numerical simulations: HEXPRESS for mesh creation, ISIS-CFD for flow solving, and CFView for result analysis. In this setup, the mesh was generated using the C-Wizard plugin in combination with HEXPRESS, NUMECA dedicated grid generator [22]. C-Wizard simplifies the process by guiding users through mesh and solver parameter configurations. Grid refinement, critical in fluid dynamics simulations, plays a key role in the accuracy of outcomes. For this simulation, a medium mesh with enhanced wave field refinement was applied.

The computational domain was defined by constructing a boundary layer surrounding the ship, with the specified boundary conditions illustrated in Figure 4. The boundary layer is a crucial concept in fluid dynamics, particularly in the context of computational simulations involving naval architecture [23]. It refers to the thin layer of fluid that is affected by the presence of a solid boundary, in this case, the ship's hull. Within this boundary layer, the effects of viscosity become significant, leading to velocity gradients and changes in flow characteristics that are critical for understanding how the fluid interacts with the surface of the ship. The dimensions of this boundary layer are carefully set based on the water length of the ship's hull (Lwl) to ensure accurate simulation [24]. Specifically, the domain extends 1 Lwl ahead of the hull, 3 Lwl behind it, 5 Lwl on each side, 1 Lwl above the hull, and 1.5 Lwl below the keel of the model. This setup facilitates a comprehensive analysis by allowing for an adequate flow region around the vessel, which is essential for achieving reliable and precise computational results in high-quality simulations.

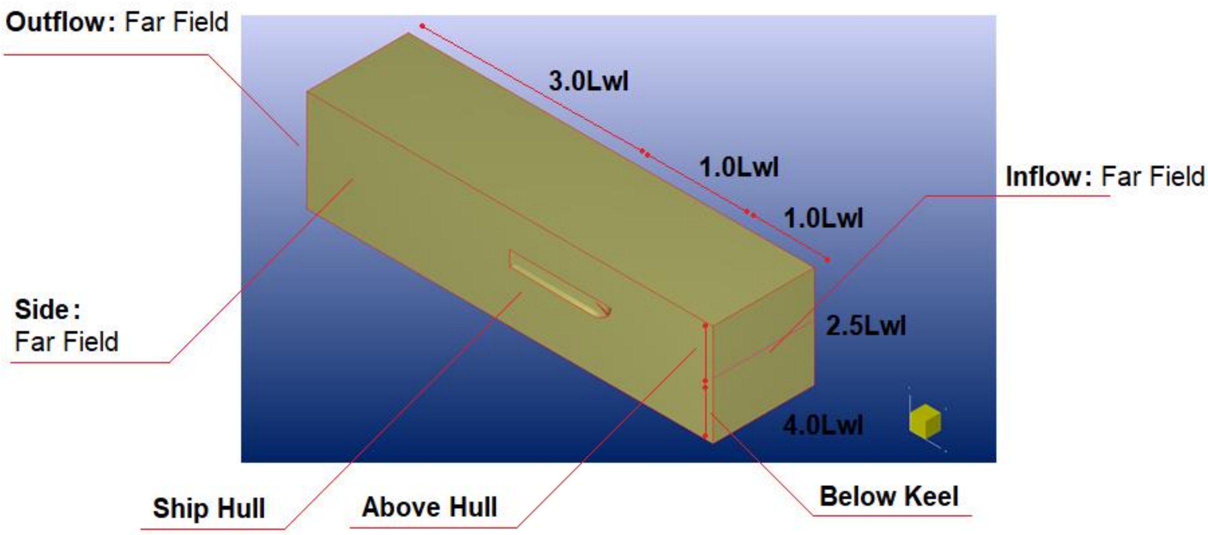

Figure 4. Domain and Boundary Layer Setup.

Primary Dimensions of the Vessel

The Method of Effect of Length on Resistance is an analytical approach that involves systematically measuring the total resistance (R_T) experienced by a ship, expressed in pounds-force (lbf), as it navigates through water, while simultaneously assessing the ship's length in feet, as these two parameters are critical in understanding the performance dynamics of the vessel. See Figure 5.

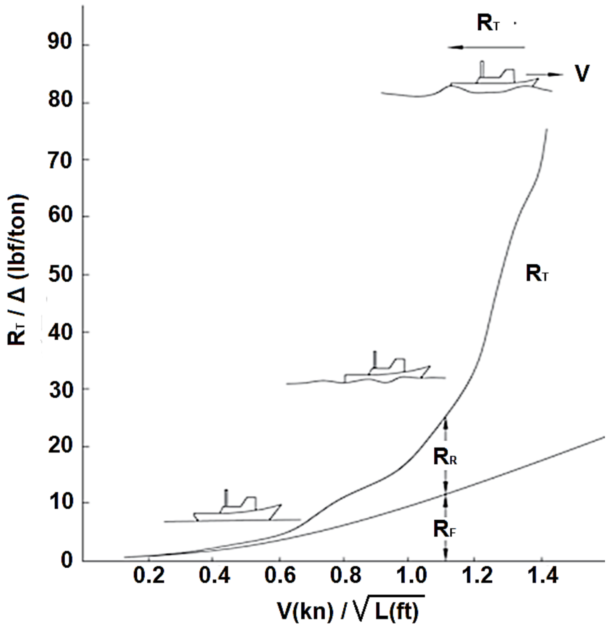

Figure 5. Typical Total Resistance per Ton Displacement Curve [25]

According to the assumptions outlined by W. Froude (1873), the total resistance R_T experienced by a ship with a wetted surface area consists of two main components: the frictional resistance R_F and residuary resistance R_R, which includes additional resistive forces such as wave-making and other effects not directly related to friction [26].

Specifically, the method entails obtaining the total resistance by conducting tests under varying conditions and at different speeds, thereby allowing for the observation of how resistance fluctuates with speed, and then calculating the resistance-to-displacement ratio by dividing the total resistance by the ship's displacement, which is measured in tons and represents the total weight of the ship, including cargo and fuel, thus yielding a more comprehensive understanding of the vessel's efficiency relative to its size; additionally, the ship's length is factored into this analysis by employing a ratio of the vessel speed (V_S) to the square root of its overall length (L), as this mathematical relationship helps elucidate the impact of length variations on resistance, thereby enabling the authors to analyze the collected data through graphical representations and mathematical models to determine optimal ship dimensions that minimize resistance and enhance operational efficiency, based on that calculation, an average value of 4181.1757 [R_T (lbf)/Displ (ton)] was obtained. This value will serve as a basis for selecting the main dimensions of the reference boat for the design..

The author analyzed six sister ships with lengths ranging from 12 to 17 meters, to assess their suitability for this research. This analysis involved calculating two critical ratios for each vessel: the resistance-to-displacement ratio, R_T (lbf)/Discp (ton), which provides insight into the ship's resistance relative to its weight, and the speed-to-length ratio, V_S (kN)/√L (ft), an indicator of performance efficiency. These values are presented in Table 1.

Table 1. Resistance and Speed Ratios.

Sister Ship Name	R_T (lbf)	Displacement (ton)	V_S (kN)	Length (ft)	R_T (lbf)/Displ (ton)	V_S (kN)/√L (ft)
Ouner	22930	4.50	20	35	5086	3.39
Angloco	253799	26.26	40	43	5029	3.78
Los Angeles	48332	9.60	27	51	2927	4.49
Crowland Pordland	119369	40.80	28	39	4480	5.03
Dock Stavarvet	149717	33.40	36	51	8828	5.77
Sea boat	162081	18.40	38	43	9665	6.10

Using the Effect of Length on Resistance as a comparative framework, the author ultimately identified the Crowland Portland (no-chine hull) as the optimal sister ship for this research due to its favorable principal dimensions and total resistance per ton displacement characteristics, detailed in Table 2.

Table 2. Ship Principal Dimensions of Selected Sister Ship (Crowland Portland).

Name of Dimensions	Dimensions Value	Units
LOA (Length of All)	16.50	m
LPP (Length Between Perpendiculars)	15.58	m
B (Beam or Breadth)	4.90	m
H (Depth)	2.50	m
T (Draft)	0.90	m
Cb (Block Coefficient)	0.479	
R_T (Total Resistance)	67.12	kN

Hull Model

Once the principal dimensions of the ship meet the required ratio criteria, a hull model of the vessel is developed. This modeling process is essential to ensure that the coefficient and dimensions values closely match or equal the target values obtained in the initial calculations, as these coefficients and dimensions are fundamental in predicting the vessel's hydrodynamic performance accurately.

Based on the body plan of a selected sister ship, the authors developed four unique hull designs to evaluate and compare the resistance and stability characteristics essential for a firefighting boat. The chine angle and number of chines were chosen to optimize resistance, as the vessel needs to achieve high speeds in the water. Each design variation aims to identify the most effective configuration by minimizing resistance while maximizing stability under operational conditions. Detailed specifications of these hull variations, including key dimensions and design features, are presented in Table 3 and Figure 6, illustrating the comparative performance criteria used in this study [27].

Table 3. Specifications of Hull Design Variations.

Name of Hull Design Variations	Number of Chine	Chine Angle (deg)	Height from Baseline (m)
Variation 1	Single Chine	0^o	0.55
Variation 2	Single Chine	10^o	0.55
Variation 3	Single Chine	17^0	0.55
Variation 4	Double Chine	0^o	0.55 and 0.65

In Variation 4, the hull design is configured with a Double Chine structure, featuring a 0° chine angle. This double chine setup results in two distinct chine heights measured from the baseline of the hull. The first chine is positioned at 0.55 meters above the baseline, while the second chine is slightly higher, at 0.65 meters from the baseline.

This arrangement is intended to influence both the resistance and stability characteristics of the hull. The chine structure plays a significant role in managing the water flow along the hull's surface, which may help reduce drag as the boat moves through the water. While the impact of the chine on stability is still under investigation, it is hypothesized that the chine may affect the boat's behavior in waves and during turns. By potentially promoting smoother water flow along the hull, the chine could contribute to improved control and lessen the chances of rolling or pitching, particularly at higher speeds.

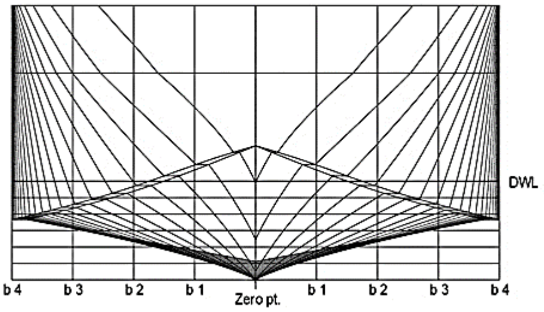

(a) Hull Variation 1

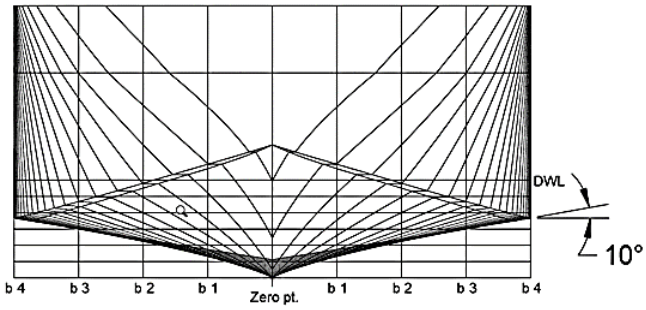

(b) Hull Variation 2

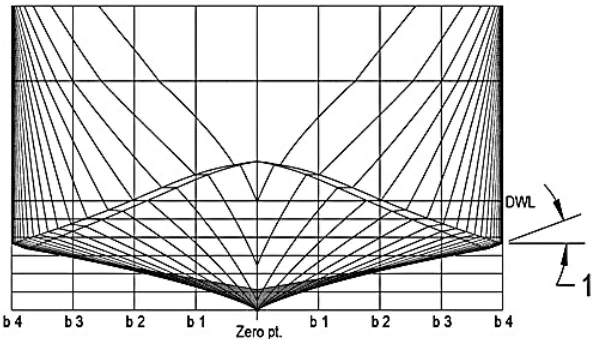

(c) Hull Variation 3

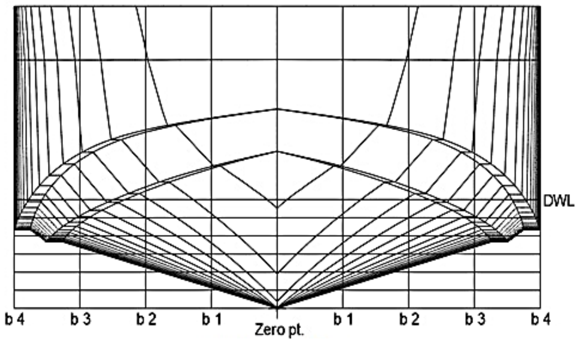

(d) Hull Variation 4

Figure 6. Hull Design Variations Included Double Chine

RESULTS AND DISCUSSION

The analysis conducted at this stage focuses on comparing the resistance values of the boat model using Maxsurf Resistance software and NUMECA Fine Marine (CFD). Resistance values for the vessel are determined through an analysis performed with Maxsurf Resistance software, which employs the Savitsky planning method to calculate these values accurately [28], [29], [30]. The criteria for the simulation specify a vessel speed of 36 knots and a corresponding Froude Number of 1.45, which are critical parameters for assessing the hydrodynamic performance of the vessel.

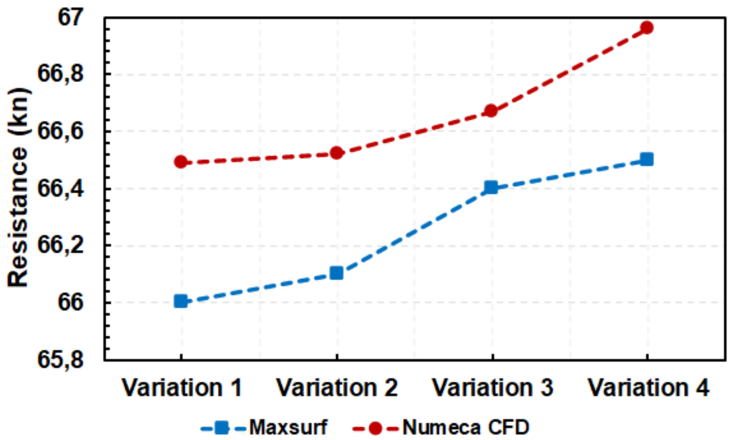

Figure 7. The Resistance Result

The analysis of resistance reveals that the variations between the results obtained from NUMECA Fine Marine (CFD) and Maxsurf Resistance software are remarkably low, with a maximum difference of 0.74% and a minimum difference of 0.4%. This close correlation indicates a high degree of consistency and reliability in the simulation results, suggesting that both computational methods yield comparable resistance values for the hull designs evaluated. On the other hand, comparative analysis reveals that the no-chine hull generates a total resistance of 67.12 kN at equivalent speeds, while the chine hull configuration, with a total resistance of 66.49 kN, demonstrates enhanced hydrodynamic efficiency.

However, it is imperative to emphasize that merely examining resistance is insufficient for identifying the most effective hull configuration. Resistance is just one facet of the vessel's performance; stability is equally critical in ensuring safe and efficient operations, especially at higher speeds [31]. Therefore, a thorough stability analysis is warranted to assess the hull's behavior under various operational conditions, including its response to external forces such as waves and wind.

A comprehensive stability analysis must be conducted to evaluate the dynamic performance of the hull designs, ensuring that our assessment encompasses all relevant aspects of maritime performance. This holistic approach will help identify the optimal hull design, one that minimizes resistance while maximizing stability and safety during operation.

Stability Analysis for Hull Selection

The stability analysis in this study aims to ensure that the designed vessel achieves stable equilibrium and can return to its upright position after experiencing angular displacement under varying load conditions and compartment configurations. Stability calculations were conducted using Maxsurf Stability software, applying criteria from the IMO A.749 (18) Code on Intact Stability [32].

Prior to performing the stability analysis, a detailed general arrangement plan was developed to define the vessel's layout. This plan is essential for the strategic placement of tanks and compartments to optimize the vessel's stability. The general arrangement includes detailed views of the vessel's layout from multiple perspectives, such as top view, side profile, and layouts of the Main Deck and passenger accommodation areas.

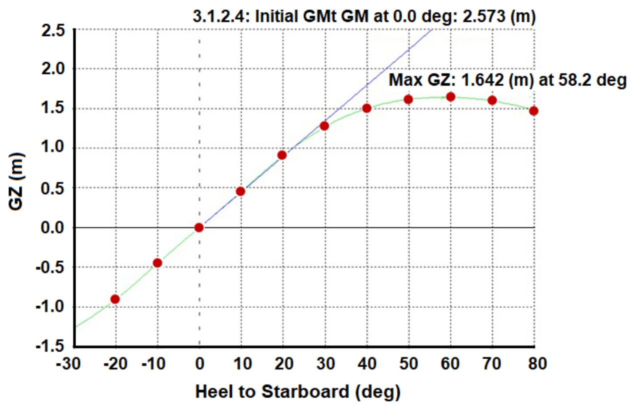

(a) GZ Curve Variation 1

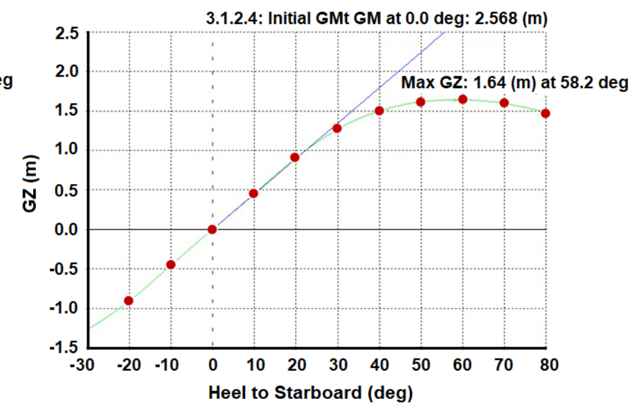

(b) GZ Curve Variation 2

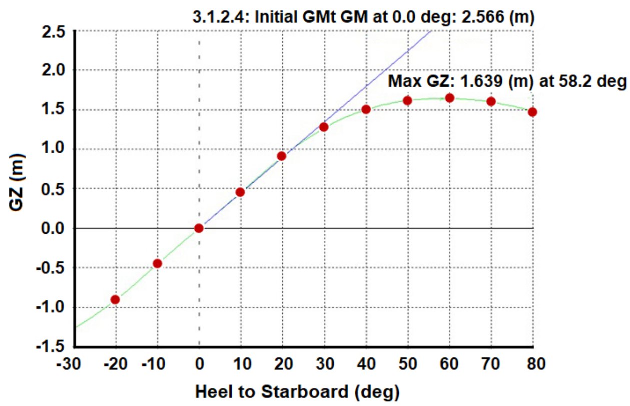

(c) GZ Curve Variation 3

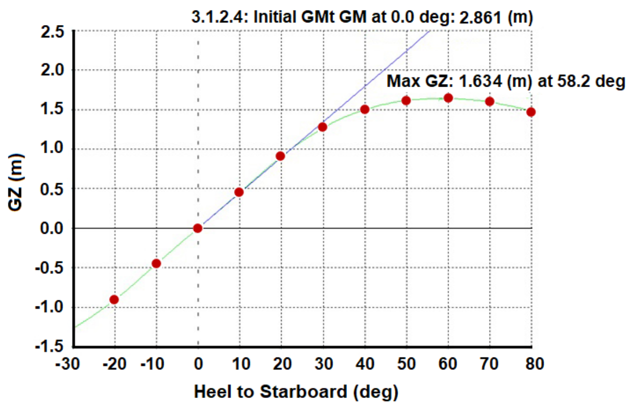

(d) GZ Curve Variation 4

Figure 8. The GZ Curve of Hull Variation Result

Table 4. Comparison of Simulation Results with IMO Criteria.

Name of GZ Curve Criteria	Variation 1	Variation 2	Variation 3	Variation 4	IMO Criteria	Result
Max GZ at 30 or Greater (m)	1.642	1.640	1.639	1.634	> 0.200 m	Pass
Angle of Max GZ (deg)	58.2^0	58.2^0	58.2^0	58.2^0	$> 25^0$	Pass
Initial GMt (m)	2.573	2.568	2.566	2.861	> 0.150 m	Pass
Rolling Period (s)	2.501	2.504	2.505	2.372		

The term Initial GMt (Transverse Metacentric Height) represents a critical measurement in assessing a ship's stability and is defined as the distance between the center of gravity (G) and the metacenter (M) of the vessel [33]. This measurement directly influences how the ship will respond to inclining forces, such as waves, wind, and other forces that cause the vessel to roll or pitch. In essence, a higher GMt typically signals greater stability, meaning the ship will resist rolling and return to an upright position more readily after inclining. Conversely, a lower GMt might indicate that the ship could experience a more pronounced rolling motion, potentially making it less stable in rough conditions.

The ship's intended operating conditions should also influence the choice of GMt. For instance, a higher GMt, such as 2.861 m, might be preferable if the vessel is expected to navigate in rough seas, as it provides a robust stability margin to counteract rolling. However, in calmer waters or when prioritizing passenger comfort, a moderate GMt, such as 2.566 m, would allow for gentler, slower rolling, which can be less jarring and improve comfort. Given the calm water conditions around the Seribu Islands, a GMt value of 2.566 m was selected, resulting in a rolling period of 2.505 seconds. Consequently, hull variation 3 will be chosen for further analysis.

Stability Analysis of Nozzle Firemonitor Placement Variations (Based on Hull 3 Design)

To achieve an even keel position, adjustments have been made to the arrangement of key components, including the fuel oil tank, fresh water tank, and main engine. This chapter focuses specifically on analyzing the placement of the fire monitor and its piping system, with particular attention to hull variation 3. Following the selection of the hull form and appropriate tank configurations, a further stability analysis will be performed, based on the variations in fire monitor nozzle placement as outlined in Figure 9. The goal of this analysis is to assess how the addition of the fire monitor affects stability, focusing on the configuration that yields the shortest rolling period. This analysis is similar to the hull selection assessment but incorporates the influence of the superstructure and fire monitor placement. The hydraulic system is selected with a single pump that has a capacity of 474 m³/h and a total head of 76.3 m, providing a spray range of 25 m for the fire monitor.

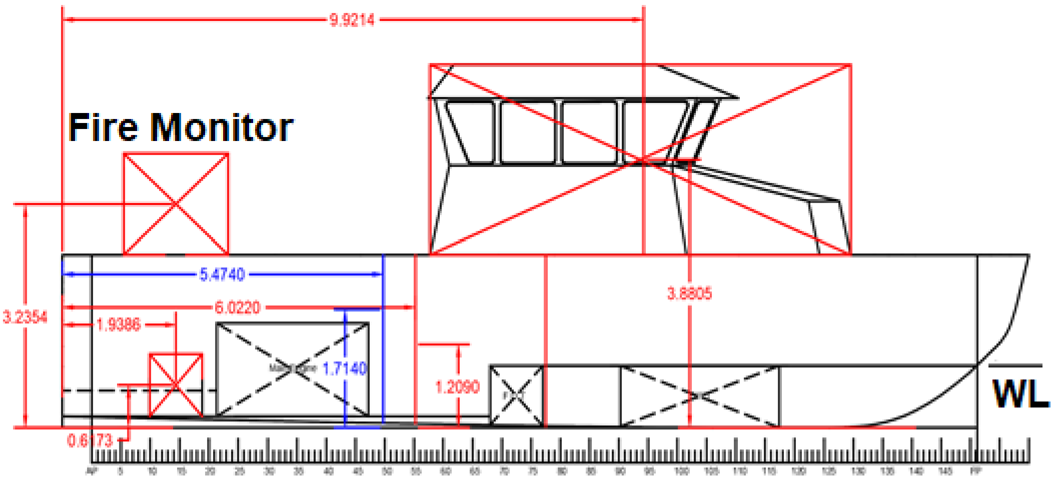

(a) Location of Aft Fire Monitor Nozzle

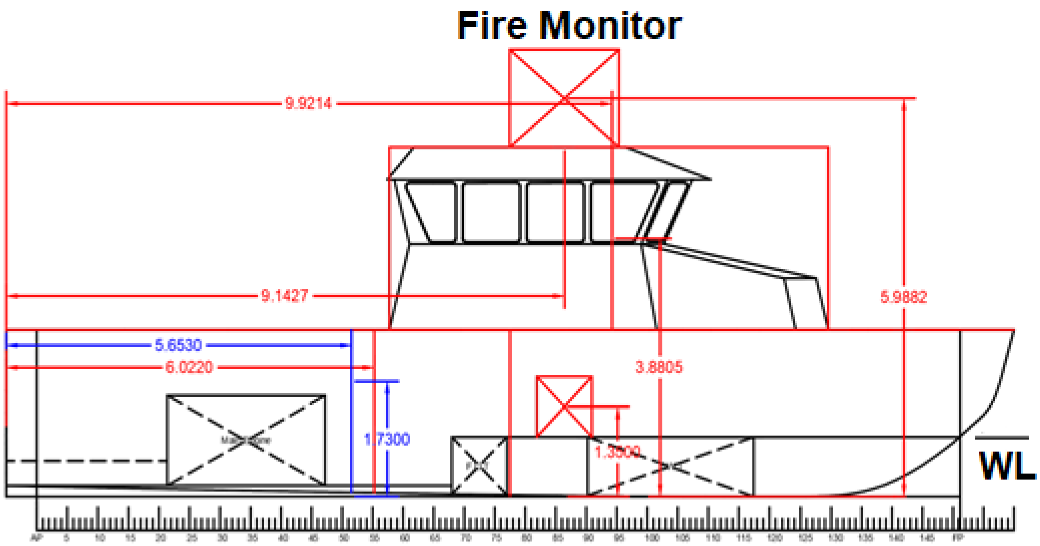

(b) Location of Midship Fire Monitor Nozzle

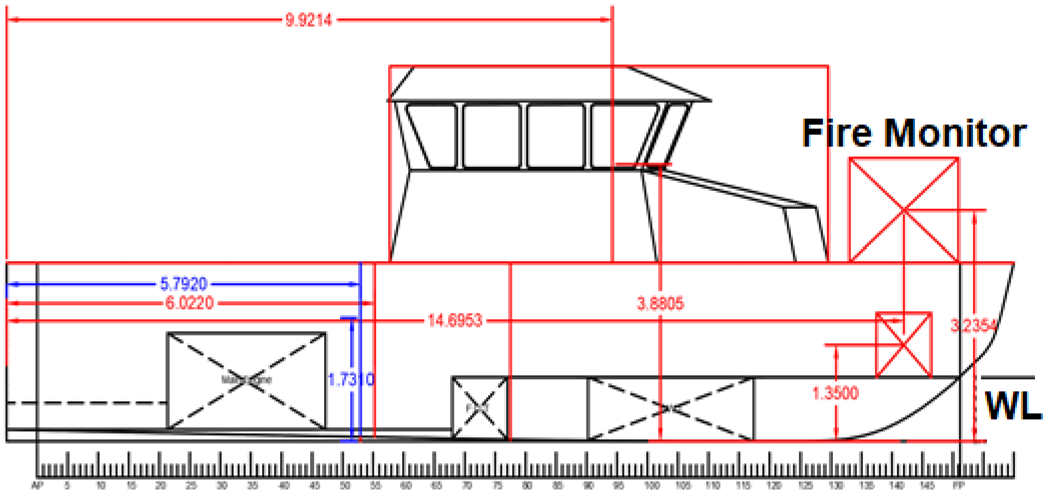

(c) Location of Forward Fire Monitor Nozzle

Figure 9. Location of Fire Monitor Nozzle Variation

After determining the vessel's total weight at the 100% Load Case, as shown in Table 5, Table 6, and Table 7, which includes for the weights of the tanks and piping linked to the fire monitor system, the authors proceeded with a stability analysis. This analysis utilized the previously mentioned weights as critical input parameters.

Table 5. Load Case Aft Fire Monitor Nozzle.

Item Name	Quantity	Unit Mass Ton	Total Mass Ton	Long. Arm (m)	Trans. Arm (m)	Vert. Arm (m)
Light Ship	1	18.45	18.45	5.474	0	1.710
Hfo	100%	2.103	2.103	7.572	0	0.587
Engine 1	1	3.270	3.270	3.929	1.225	0.840
Engine 2	1	3.270	3.270	3.929	-1.225	0.840
Fw Tank	100%	6.244	6.244	10.419	0	0.595
Fire Monitor	1	0.050	0.050	1.939	0	3.139
Pump	1	0.410	0.410	1.939	0	0.436
Total Loadcase			33.8	6.171	0	1.253

Table 6. Load Case Midship Fire Monitor Nozzle.

Item Name	Quantity	Unit Mass Ton	Total Mass Ton	Long. Arm (m)	Trans. Arm (m)	Vert. Arm (m)
Light Ship	1	18.455	18.455	5.653	0	1.730
Hfo	100%	2.103	2.103	7.572	0	0.587
Engine 1	1	3.270	3.270	3.929	1.225	0.840
Engine 2	1	3.270	3.270	3.929	-1.225	0.840
Fw Tank	100%	6.244	6.244	10.419	0	0.595
Fire Monitor	1	0.050	0.050	9.143	0	5.892
Pump	1	0.410	0.410	9.143	0	1,350
Total Loadcase			33.8	6.367	0	1.277

Table 7. Load Case Forward Fire Monitor Nozzle.

Item Name	Quantity	Unit Mass Ton	Total Mass Ton	Long. Arm (m)	Trans. Arm (m)	Vert. Arm (m)
Light Ship	1	18.455	18.455	5.791	0	1.727
Hfo	100%	2.103	2.103	7.572	0	0.587
Engine 1	1	3.270	3.270	3.929	1.225	0.840
Engine 2	1	3.270	3.270	3.929	-1.225	0.840
Fw Tank	100%	6.244	6.244	10.419	0	0.595
Fire Monitor	1	0.410	0.410	14.695	0	1.350
Pump	1	0.050	0.050	14.695	0	3.235
Total Loadcase			33.80	6.518	0	1.271

In our analysis, we focused on the 100% load case because it represents the vessel's maximum operational weight, which is especially crucial for firefighting and emergency response vessels equipped with heavy onboard systems like fire monitors. In these vessels, the 100% load case provides a comprehensive picture of stability under the heaviest possible configuration, where all fuel, water, firefighting equipment, and other resources are fully loaded.

Furthermore, the measured values of the Longitudinal Center of Gravity (LCG) and Vertical Center of Gravity (VCG) were also incorporated as essential inputs for the stability assessment, thereby ensuring a thorough evaluation of the vessel's stability characteristics. Figure 10 presents the updated GZ values derived from the stability analysis simulations performed at the aft, midship, and forward positions of the fire monitor nozzle.

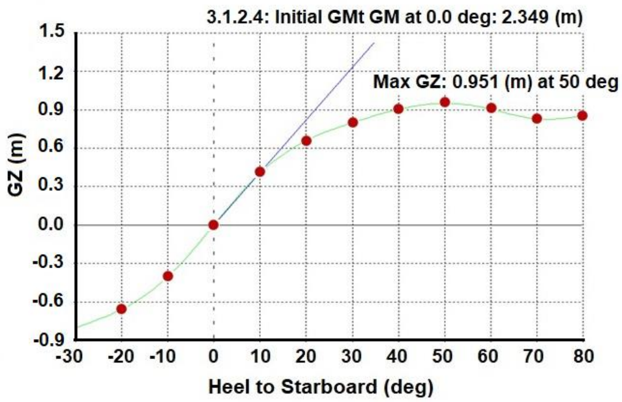

(a) GZ Curve Aft Fire Monitor Nozzle

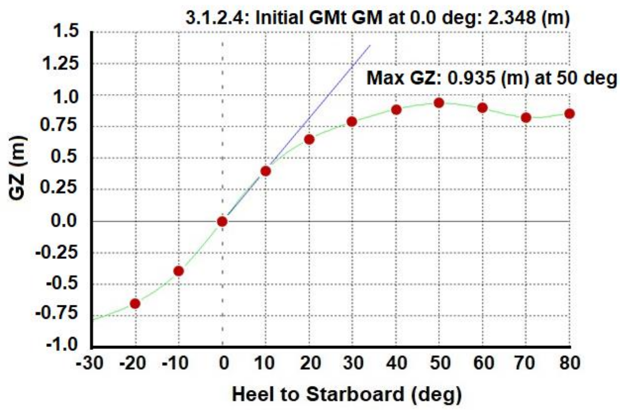

(b) GZ Curve Midship Fire Monitor Nozzle

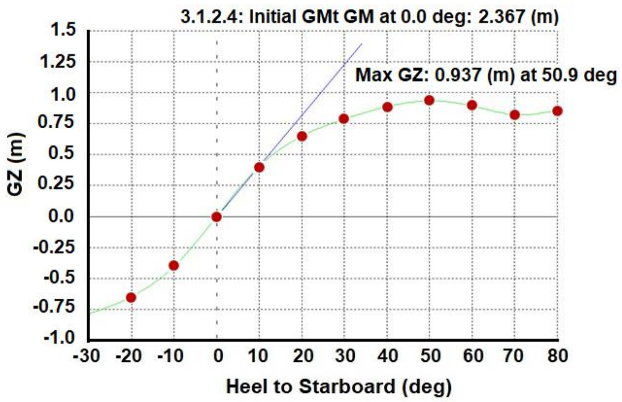

(c) GZ Curve Forward Fire Monitor Nozzle

Figure 10. The GZ Curve of Fire Monitor Nozzle Variation

Table 8. Simulation Results of Optimal Fire Monitor Positioning.

Monitor Nozzle Placement Variation	Max GZ (deg)	Vessel Rolling Period (Seconds)	Vessel Trim (m)
Aft Fire Monitor Nozzle	50º	3,140	0
Midship Fire Monitor Nozzle	50º	3,142	-0,109
Forward Fire Monitor Nozzle	50,9º	3,128	-0,191

This selection focuses on the impact of fire monitor placement on the resulting vessel trim. As indicated in Table 8, the aft-positioned fire monitor nozzle yields a trim value of zero, achieving an even keel condition (with the fore and aft draft levels balanced) in comparison to other configurations. This configuration offers a maximum GZ value of 50 degrees, indicating a strong righting moment, and a rolling period of 3.140 seconds, which falls within an acceptable range for stability and operational comfort. Based on these findings, the aft placement of the fire monitor nozzle emerges as the optimal choice, as it not only maintains an even keel but also meets stability criteria effectively. This configuration is therefore recommended for its balanced performance in terms of both trim and stability parameters. Figure 11 presents the 3D model of the firefighting system, designed with an aft-positioned fire monitor optimized for the coastal conditions of the Seribu Islands.

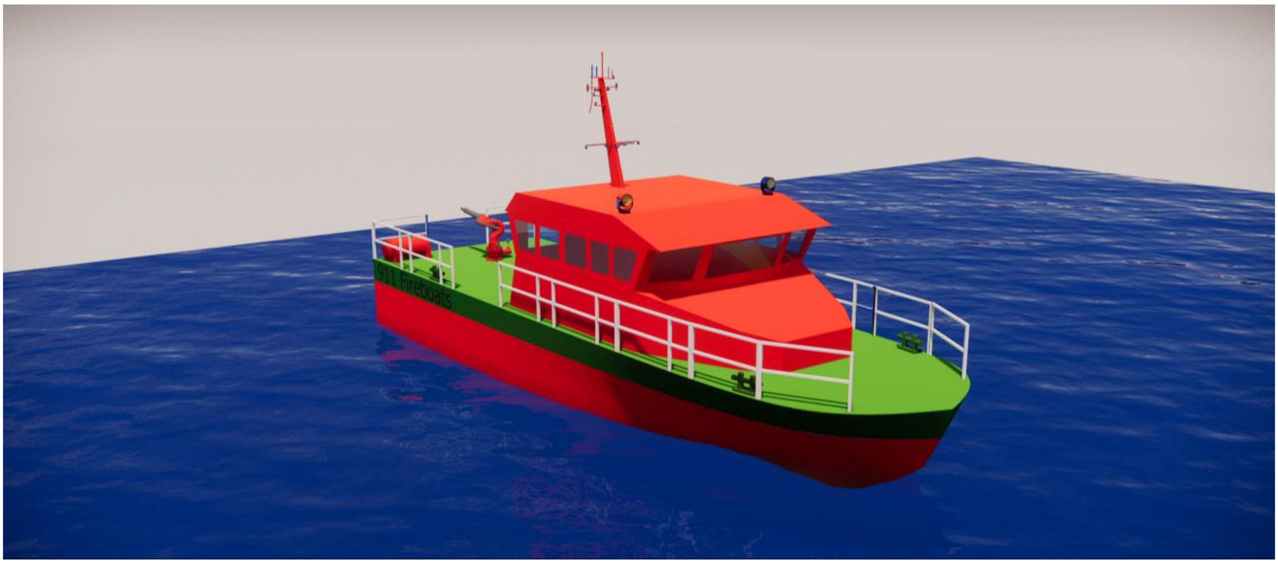

Figure 11. 3D Firefighting Boat Model with Aft-Positioned Fire Monitor

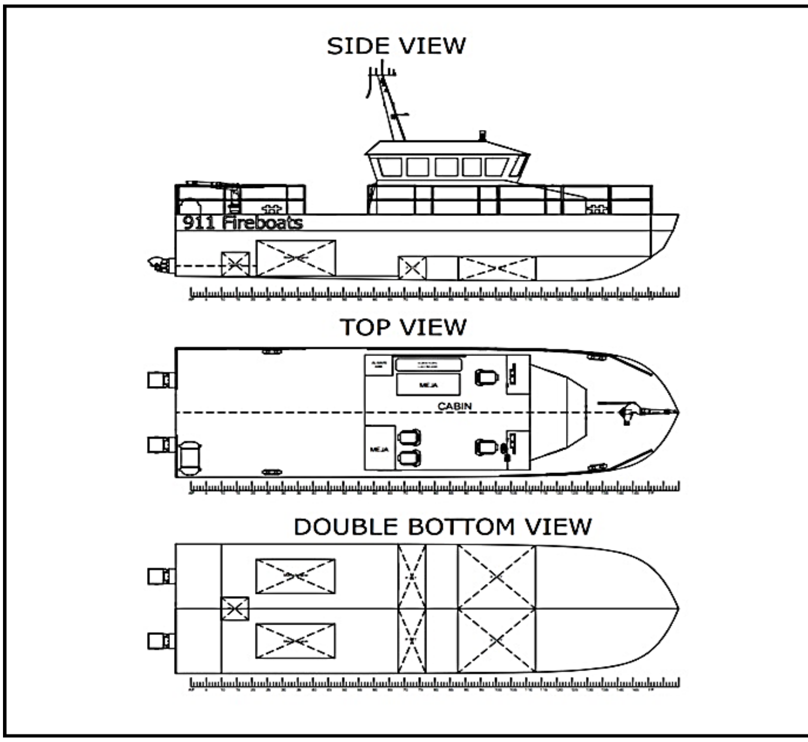

Principal Dimensions			
Dimension Names		Value	Unit
1	LOA	16,5	m
2	LPP	15,588	m
3	LWL	15,6076	m
4	B	4,9	m
5	H	2,5	m
6	T	0,9	m
Design Parameters			
7	Vs	36	Knot
8	Cb	0,479	
9	Cp	0,755	
10	Displacement	33,81	ton
11	Volume Displacement	32,989	m^3

Figure 12. General Arrangement of Firefighting Boat Model with Aft-Positioned Fire Monitor.

CONCLUSION

The analysis conducted reveals several key findings that address the objectives of the research. First, the size and design parameters for Hull Variation 3, selected through total resistance per ton displacement curve, yield optimal hydrodynamic efficiency for the designed firefighting vessel. Second, the hydraulic system is selected with a single pump capacity of 474 m^3/h and a total head of 76.3 m, ensuring a spray range for the fire monitor of 25 m, which supports effective firefighting operations. Finally, stability analysis indicates that the placement of the fire monitor nozzle at the aft results in a balanced trim, achieving a maximum GZ value of 50 degrees and a rolling period of 3.140 seconds. These findings suggest that this configuration enhances stability and ensures operational safety during firefighting activities. Overall, this research highlights the critical relationship between hydrodynamic performance and stability in the design of firefighting vessels, providing a foundation for further exploration of optimal vessel configurations to enhance effectiveness and safety in maritime firefighting operations.

ACKNOWLEDGEMENT

The authors would like to express their sincere gratitude to the colleagues of Ship Design Laboratory, Ship Manufacturing Engineering and Department of Naval Architecture, Institut Teknologi Sepuluh Nopember for their invaluable support and assistance throughout the course of this research. Their extensive resources, expertise, and unwavering guidance have significantly contributed to the success of this project. We are truly thankful for the opportunity to collaborate with such dedicated professionals, whose insights and encouragement have been instrumental in advancing our work and achieving our research objectives.

REFERENCES

[1]. Farhan, A.R. and Lim, S., 2012. Vulnerability assessment of ecological conditions in Seribu Islands, Indonesia. Ocean & coastal management, 65, pp.1-14.

[2]. Goni, J.I. and Yustika, B.P., 2019. The presence of global value chain in coastal marine tourism. Jurnal Riset Manajemen Dan Bisnis (JRMB) Fakultas Ekonomi UNIAT, 4(1), pp.137-152.

[3]. Akten, N., 2006. Shipping accidents: a serious threat for marineenvironment. Journal of Black Sea/Mediterranean Environment, 12(3), pp.269-304.

[4]. Sardar, A., 2024. Improving safety and efficiency in the maritime industry: a multi-disciplinary approach (Doctoral dissertation, University of Tasmania).

[5]. Wang, H., Boulougouris, E., Theotokatos, G., Priftis, A., Shi, G., Dahle, M. and Tolo, E., 2020. Risk assessment of a battery-powered high-speed ferry using formal safety assessment. Safety, 6(3), p.39.

[6]. Darma, Y.Y.E., Pratama, R.H., Yudha, I.S.P.D. and Kusuma, A.I., 2024. Impact of Stepped Hull Design on Speed Boat Performance: A CFD Study. Evergreen, 11(3), pp.2580-2589.

[7]. Ramadhani, B., Darma, Y.Y.E., Prasetya, I.S. and Arifin, M.D., 2023. Hydrostatics Curve Approach as a Design Development of Fishing Canoe With Bilge Keel to Improve Rolling Period. International Journal of Marine Engineering Innovation and Research, 8(2).

[8]. Darma, Y.Y.E., Inprasetyobudi, H., Utomo, R.E.P., Wibowo, G.H., Hidayat, A. and Saragih, A.D., 2023. Motions Analysis Investigation of a 12 Meter Catamaran Tourism Boat on Passenger Comfort Criteria Case Study" MV Garuda Ngelayang. International Journal of Marine Engineering Innovation and Research, 8(2).

[9]. Allan, R.G., Harford, K.D., Noon, D., Bjerkeset, J., Dalton, J. and Siegel, W., 2010, November. Concept Development, Detailed Design and Construction of the Three Forty Three–North America's Most Powerful Fireboat. In SNAME Maritime Convention (p. D031S006R002). SNAME.

[10]. Gao, D., Xie, W., Bao, C., Liu, B. and Zhuang, J., 2023. A Control Method for Water Cannon of Unmanned Fireboats Considering Wind and Ship Motion Disturbances. Journal of Marine Science and Engineering, 11(2), p.445.

[11]. A. Lindholdt, K. Dam-Johansen, S.M. Olsen, D.M. Yebra, and S. Kiil, “Effects of biofouling development on drag forces of hull coatings for ocean-going ships: a review,” J Coat Technol Res, 415–444 (2015). doi:10.1007/s11998-014-9651-2.

[12]. R. Cooke, “An experimental investigation into the components of ship resistance,” University of Cape Town, 1986.

[13]. M.F. Syahrudin, M.A. Budiyanto, and M.A. Murdianto, “Analysis of the use of stern foil on the high speed patrol boat on full draft condition,” Evergreen, 7 (2) 262–267 (2020). doi:10.5109/4055230.

[14]. A.F. Molland, S.R. Turnock, and D.A. Hudson, “Ship Resistance and Propulsion: Practical Estimation of Propulsive Power,” Cambridge University Press, Cambridge, 2011. doi:DOI: 10.1017/CBO9780511974113.

[15]. Edward V. Lewis, “Principles of Naval Architecture,” SNAME, 1988.

[16]. Ziylan, K. and Nas, S., 2022. A Study on the Relationship Between Ship Resistance and Trim, Supported by Experimental and Software-Based Analysis. Transactions on Maritime Science, 11(02), pp.5-5.

[17]. H. Anam, L. Haris, A. Budiyarto, and A. Budiyono, “Design of diver propulsion vehicle ganendra ri-1 using solidworks flow simulation,” Marine and Underwater Science and Technology, 1 55–60 (2015).

[18]. Y. Cui, J. Ravnik, O. Verhnjak, M. Hriberšek, and P. Steinmann, “A novel model for the lift force acting on a prolate spheroidal particle in arbitrary non-uniform flow. part ii. lift force taking into account the non-streamwise flow shear,” International Journal of Multiphase Flow, 111 232–240 (2019). doi:https://doi.org/10.1016/j.ijmultiphaseflow.2018.12.003.

[19]. Gao, D., Xie, W. and Wang, Y., 2023. A control method for water cannon of unmanned fireboats based on EGWO-ADFUZZY. Ocean Engineering, 289, p.116237.

[20]. Nam-Kyun, I.M. and Hun, C.H.O.E., 2021. A quantitative methodology for evaluating the ship stability using the index for marine ship intact stability assessment model. International Journal of Naval Architecture and Ocean Engineering, 13, pp.246-259.

[21]. Chiroşcă, A.M. and Rusu, L., 2021. Comparison between model test and three CFD studies for a benchmark container ship. Journal of Marine Science and Engineering, 9(1), p.62.
[22]. Pacuraru, F., Domnisoru, L. and Pacuraru, S., 2020. On the comparative seakeeping analysis of the full scale KCS by several hydrodynamic approaches. Journal of Marine Science and Engineering, 8(12), p.962.
[23]. Gad-el-Hak, M., 1994. Interactive control of turbulent boundary layers-A futuristic overview. AIAA journal, 32(9), pp.1753-1765.
[24]. Kleinsorge, L., Lindner, H. and Bronsart, R., 2016. A Computational Environment for Rapid CFD Ship Resistance Analyses. Proceedings of PRADS2016, 4, p.8th.
[25]. Papanikolaou, A., 2014. Ship design: methodologies of preliminary design. Springer.
[26]. Froude, W., 1873. Apparatus for Automatically Recording the Rolling of a Ship in a Sea-Way, and the Contemporaneous Wave-Slopes. Royal United Services Institution. Journal, 17(75), pp.858-887.
[27]. Hidayat, A., Inprasetyobudi, H. and Darma, Y.Y.E., 2021. Design and modeling of catamaran flat plate ship with bottom glass concept to improve tourism underwater in Bangsring Banyuwangi. Kapal: Jurnal Ilmu Pengetahuan dan Teknologi Kelautan, 18(3), pp.140-150.
[28]. Arifin, M.D., Felayati, F.M., Muslim, M., Buwono, A. and Darma, Y.Y.E., 2023. Numerical Study of Kaplan Propeller by Using CFD: Effect of Angle and Blade Diameter Variations. International Journal of Marine Engineering Innovation and Research, 8(2).
[29]. Wahyudin, I., ED, Y.Y., Prasetya, I.S. and Insprasetyobudi, H., 2022. Preliminary Design of Traditional Fishing Boat (2 GT) With Additional Floating Compartment for Safety Reasons Using BKI Rules. International Journal of Marine Engineering Innovation and Research, 7(4).
[30]. Darmawan, A.B., Darma, Y.Y.E. and Rulianto, J., 2022, September. Analysis The Effect of Outrigger (Cadik) Variations on Motion Response of Fishing Boat Using CFD Method. In IOP Conference Series: Earth and Environmental Science (Vol. 1081, No. 1, p. 012010). IOP Publishing.
[31]. Geertsma, R.D., Negenborn, R.R., Visser, K. and Hopman, J.J., 2017. Design and control of hybrid power and propulsion systems for smart ships: A review of developments. Applied energy, 194, pp.30-54.
[32]. Islam, M.R., Barnil, A.S.H., Rahman, M.S. and Hossain, K.A., 2022. Applicability of Current Statutory Rules for Stability Requirements of Bangladesh Inland Passenger Vessels. Journal of Ship Research, 66(03), pp.219-230.
[33]. Lee, B.S., 2019. Hydrostatics and Stability of Marine Vehicles. Springer Singapore.